Moisture Buffer Capacity of Different Insulation Materials

Ruut Peuhkuri, Ph.D. **Carsten Rode, Ph.D.** *Member ASHRAE* **Kurt Kielsgaard Hansen, Ph.D.**

ABSTRACT

There is an increasing focus on the possibilities of utilizing the absorptive ability of porous materials to create passive control of humidity variations in the indoor air. These variations result in peaks in the indoor air humidity due to moisture production or in the exterior building envelope due to the diurnal variations of outdoor air temperature and humidity. Passive control of the humidity of the indoor air—particularly together with passive thermal control—may lead to smaller energy use for climatization of buildings. For exterior envelopes, the choice of the right materials can lead to more durable constructions.

This paper describes the testing of a large range of very different thermal insulation materials in specially constructed laboratory facilities to determine their moisture buffer capacity. Both isothermal and non-isothermal experimental setups have been used. In the isothermal tests the material samples were exposed to the same change in the relative humidity of the ambient air on both sides, while the samples were exposed to variations in relative humidity only on the cold side in the non-isothermal tests.

The results of these rather different measurement principles are discussed, and different ways are presented to determine the moisture buffer capacity of the materials using partly standard material parameters and partly parameters determined from actual measurements.

The results so far show that the determination of moisture buffer capacity is very sensitive to the method of analysis used and, therefore, great care has to be taken when comparing results of different experiments. The paper discusses this issue and recommends a simple and consistent way to present the moisture buffer capacity of the materials in contact with the indoor air on the basis of experimental results.

INTRODUCTION

There is an increasing focus on the possibilities of utilizing the absorptive ability of porous materials to create passive control of humidity variations in the indoor air. These variations can result in peaks in the indoor air humidity due to moisture production or in the exterior building envelope due to the diurnal variations of outdoor air temperature and humidity. Passive control of the humidity of the indoor air—particularly together with passive thermal control—may lead to smaller energy use for climatization of buildings. For exterior envelopes, the choice of the right materials can lead to more durable constructions. So in order both to characterize the performance of building materials to exchange moisture with the climate that surrounds them and to characterize their intrinsic immunity against moisture impacts, a term such as *moisture buffer capacity* could be beneficial.

As a supplement to using experience and sensible judgment in the design process, numerical simulations may be helpful to specify the materials in the right way. The aim of hygrothermal simulations of building envelopes is normally to predict how the designed construction will perform when exposed over extended periods to naturally varying temperature and moisture loads. The materials are represented in the simulation models by their measured moisture properties. Although the boundary conditions used are dynamic, the common simulation models assume that there exists local

Ruut Peuhkuri is an assistant research professor and **Carsten Rode** and **Kurt Kielsgaard Hansen** are associate professors in the Department of Civil Engineering, Technical University of Denmark, Lyngby, Denmark.

hygrothermal equilibrium within the material. This assumption makes it possible to convert local vapor pressure to moisture content of the material via a sorption isotherm. While it is widely accepted that this assumption is not absolutely correct, for many materials the resulting error is considered small. However, the assumption of immediate local moisture equilibrium ignores a possible time delay in the sorption processes, which can introduce significant errors in modeling the effects of rapid change in the relative humidity (RH) of air.

Therefore, the central problem of these simulation models is the conflict between steady-state and equilibrium-based material properties and the dynamic boundary conditions. For instance, the water vapor permeability of porous, absorbent materials is based on steady-state measurements using the cup method. Such measurements do not involve water absorption by the material and are really just a measure of gas transmission through the physical pore structure. In practice, materials in a building envelope are exposed to naturally varying, non-isothermal conditions on both daily and annual time scales.

The existence of so-called retarded sorption has been accepted for wood as a result of several studies (e.g., Wadsö 1993; Håkansson 1998; Koponen and Liu 1999). It is not usually possible to describe this nature of materials such as wood with standard material properties. Therefore, there is a need to develop a methodology for the characterization of the dynamic response of the materials. No such methodology exists yet, but some experimental and theoretical research work already exists studying this issue.

State-of-the-Art Experimental Work on Moisture Buffer Capacity

Padfield (1999) investigated a range of different porous building materials to find their moisture buffer capacity on the indoor air humidity. A specially constructed climate chamber (about 2.5 × 2.5 × 2.5 ft) was used to measure the RH-buffering ability of different materials when there is a periodically varying vapor flux. The resulting relative humidity in the chamber was a function of both porosity and the adsorptive capacity of the material. Moisture buffering capacity was defined as a weight change of the sample as a function of the ambient RH change and measured for wood, brick, cellular concrete, and unfired clay. The setup imitated the typical combination of material area, air volume, and water production in a room. End grain wood panels showed the best buffering capacity due to the rapid diffusion and the great moisture capacity of wood. On the other hand, cellular concrete covered by a thin gypsum plaster turned out to be the best buffering commercial construction.

Mitamura et al. (2001) used a room-size test cell to investigate the moisture buffer capacity of plasterboard, chipboard, cellular concrete, plywood, wood panels, and painted plasterboard when the relative humidity of the test cell was registered as a result of given rates of moisture release and removal to/from the cell air and moisture was exchanged with the materials. The moisture buffer capacity was given as the weight change of the sample material as a function of variation in the resulting indoor air relative humidity. The highest buffer capacity was measured for wood panels and cellular concrete. The same setup was used in an investigation where the layers of an interior wall were added successively (Hedegaard 2002). The results of the experiments indicated that mineral wool has a poor moisture buffer capacity whereas the cellulose insulation has very good buffering capacity. But it was also shown that for daily variations it is not possible to take advantage of the moisture buffer capacity of the deeper layers in a composite interior wall when a plasterboard cladding is used.

An approach to developing a test method and device to test the effective moisture capacity of structures or material layers that are in contact with an air space having changing relative humidity conditions is described in Ojanen and Salonvaara (2003). The sample was placed in a chamber that has openings both to the surrounding air and to a chamber with a saturated salt solution. By opening and closing these openings, the relative humidity around the test sample can be changed stepwise to cause either wetting or drying conditions. The resulting weight change of the sample for a given time period is used as the moisture buffer capacity. Pine, different kinds of plywood, and gypsum boards were tested. The preliminary results have shown that pine with moisture transport along the grain has the highest moisture buffer capacity, while painted gypsum board has the lowest.

ANALYTICAL BACKGROUND

To understand the dynamic behavior of the materials and some main trends in the existing studies, a short introduction to moisture dynamics and a possible definition of moisture buffer capacity are given in this section.

Dynamic Moisture Transport Theory

The theory of moisture transport in porous materials is originally based on Fick's law of diffusion of ions in water (Fick 1855). This simple law is adopted in building science to describe the diffusion of water vapor in porous materials. By regarding the water vapor as an ideal gas and assuming isothermal conditions, Fick's law can be given as in Equation 1.

$$g_v = -\delta_p \frac{\partial p}{\partial x} \tag{1}$$

where g_v (kg/m^{2}s) is the water vapor flux density, δ_p (kg/(Pa·m·s)) is the water vapor permeability of the material, and $\partial p/\partial x$ (Pa/m) is the gradient of the water vapor pressure.

When setting up the theoretical model to be able to analyze the dynamic moisture transport, the governing equation for conservation of mass in a unit volume can be expressed as in Equation 2.

$$\nabla g \pm S_M = -\frac{\partial w}{\partial t} \quad (2)$$

where ∇g (kg/m^{3}s) is the divergence of moisture flux, S_M (kg/m^{3}s) is the moisture source term, w (kg/m^3) is the moisture content by volume, and t (s) is time.

Dynamic water vapor transport can be described by Fick's second law, Equation 3, when combining Equations 1 and 2, neglecting moisture source term S_M, and regarding only one-dimensional transport.

$$\frac{\partial w}{\partial t} = \frac{\partial}{\partial x}\left(\delta_p \frac{\partial p}{\partial x}\right) \quad (3)$$

The relation between the state variable w and the driving force $\partial p/\partial x$ in Equation 3 is traditionally given by the moisture capacity of the material $\partial w/\partial \varphi$ (kg/m^3), where φ is the relative humidity (-). Under assumption of isothermal conditions, the driving force in Equation 3 can be expressed by the moisture content w.

$$\frac{\partial w}{\partial t} = \frac{\partial}{\partial x}\left(\frac{\delta_p \cdot p_{sat}}{\frac{\partial w}{\partial \varphi}} \frac{\partial w}{\partial x}\right) = \frac{\partial}{\partial x}\left(D_w \frac{\partial w}{\partial x}\right) \quad (4)$$

where D_w (m^2/s) is moisture diffusivity and p_{sat} (Pa) is saturation vapor pressure. The diffusivity includes information about both the moisture transport and retention, and gives a measure of how quickly or slowly the moisture conditions in a material change under alternating ambient conditions. Not only the transport properties, but also the moisture capacity of the material plays a very important role.

As given above, the diffusivity D_w can be calculated from the permeability δ_p and moisture capacity $\partial w/\partial \varphi$ by Equation 5 or it can be determined from dynamic sorption experiments as will be shown in "Results."

$$D_w = \frac{\delta_p \cdot p_{sat}}{\frac{\partial w}{\partial \varphi}} \quad (5)$$

Theoretical Definition of Moisture Buffer Capacity

A material's ability to absorb or release moisture with the climate that surrounds it is sometimes called the *moisture buffer capacity* of the material, and it is a function of permeability and the absorptive power of the material. This ability is interesting, for example, when designing (partly) passive indoor climate regulation strategies or when studying the robustness of a construction against interstitial condensation. Following are two different ways of characterizing the moisture buffer capacity of the materials.

Moisture Accumulation Capacity. A material's ability to absorb and release heat is given by thermal effusivity b (J/(m^{2}K·s$^{0.5}$)), Equation 6.

$$b = \sqrt{\lambda \cdot \rho_0 \cdot c_p} = \frac{\lambda}{\sqrt{\alpha}} \quad (6)$$

where λ (W/(m·K)) is thermal conductivity, ρ_0 (kg/m^3) is dry density of the material, c_p (J/(kg·K)) is heat capacity, and α (m^2/s) is thermal diffusivity, which shows how fast temperature changes propagate in a material (Hagentoft 2001). The thermal effusivity can also be understood as the heat accumulation capacity of the material.

Analogous to the heat accumulation capacity of the material is the moisture accumulation capacity of a material b_m (kg/(m^{2}Pa· s$^{0.5}$)) given by Equation 7. This is not given directly, but it can be derived from the analysis in Hagentoft (2001):

$$b_m = \sqrt{\frac{\delta_p \cdot \frac{\partial w}{\partial \varphi}}{p_{sat}}} \quad (7)$$

Available Water. As a part of determination of the other way of defining the moisture buffer capacity—the available water Δm_w (kg/m^2)—it is especially important to know how much of the material is activated in the moisture buffering process. This can be expressed as the penetration depth d_p, Equation 8.

$$d_p = \sqrt{\frac{D_w \cdot t_p}{\pi}} \quad (8)$$

where t_p is the period (s).

Therefore, when assessing the moisture accumulation capacity of porous materials, diffusivity D_w plays a major role in quantifying this capacity because it is of great importance how much of the material's moisture capacity is activated under typical dynamic moisture conditions. The penetration depth d_p for a harmonic relative humidity variation on the surface of a semi-infinite material can be seen as a characterization of the active mass: d_p (m) defines the distance from the material surface where the amplitude is $e^{-1} \approx 36.7\%$ of the amplitude on the material surface. This fraction is an arbitrary but analytically elegant choice.

The penetration depth alone is not capable of describing the buffer capacity; it also depends on the amount of moisture the material is able to release or take up, i.e., the volumetric moisture capacity of the material $\partial w/\partial \varphi$ and the size of the ambient relative humidity change $\Delta\varphi$. Therefore, the resulting moisture buffer capacity can be given as the amount of available water Δm_w the material is able to release or take up during a given time period for a given change in relative humidity of the air. This is given by Equation 9, which is inspired by Padfield (1999).

$$\Delta m_w = \frac{\partial w}{\partial \varphi} \cdot \Delta\varphi \cdot d_p \quad (9)$$

EXPERIMENTS

The experimental part of the work was based on two different types of investigations: (1) isothermal, dynamic measurements of absorption and desorption steps and (2) non-isothermal dynamic measurements, where the cold side of the sample was exposed to a periodically varying RH. These two tests methods will be introduced separately in this section. Also, analysis of the results is given separately in the next section.

Isothermal Tests

For the isothermal experiments was used a micro-scale sorption apparatus, where the weight change of a micro scale specimen was followed. The aim of the experiments was to study the sorption behavior of a material when the sample was subjected to a step change in the ambient relative humidity.

Experimental Setup. The micro-scale sorption experiments were carried out with standard sorption equipment (see Figure 1). The sorption equipment has a sensitive microbalance (capacity 200 mg), which continuously registers the weight of the sample together with the temperature and relative humidity around the sample. The temperature can be varied from 5°C to 80°C and the relative humidity from 0% RH to 95% RH.

Wet and dry airstreams controlled the relative humidity while the temperature was regulated by water circulation in a kind of heat exchanger around the sample. The sample was placed within a weighing basket and positioned on the microbalance. The chamber was then closed and the sample sealed in position. Sample drying before sorption measurements was carried out at 20°C in flowing nitrogen until sample weight was in equilibrium at 0% RH, for about 12 hours. The accuracy of the equipment is given in Table 1. In this apparatus, the sample size is rather small so the results are mainly dominated by the dynamic moisture uptake by the fine pores and the pore wall constituents, e.g., cellulose.

Measurement Strategy. After drying, the sorption measurements began. The climate around the sample was held constant until equilibrium, or until a given time was exceeded, before changing the RH to the next level. Step changes of 5% RH were used, and measurements were over the range from 0% to 95% RH. The end drying was made at 50°C. The maximal time step used in these measurements was eight hours to reach equilibrium at each RH level.

Besides the standard sorption isotherm, all the continuous registrations of RH, weight, and T determined by the equipment (the kinetic data) could also be exported. These data were used in the main analysis of the results in this paper.

Non-Isothermal Tests

Completely different equipment was used for the non-isothermal experiments. The setup allows the creation of a dynamic climate on the cold side of the sample. This experimental setup is a prototype apparatus and somewhat comparable with full-scale field experiments, although in this equipment the conditions are designed and regulated. Most important also, the resulting moisture flux as well as the hygrothermal states around and within the material are monitored. The aim of these actual measurements is to identify the dynamic moisture response of a material exposed to also a temperature gradient.

(a)

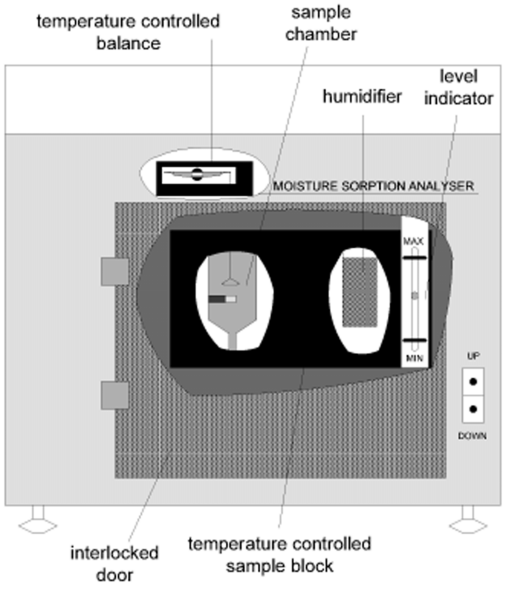

(b)

Figure 1 *The sorption equipment: (a) overall photo, (b) drawing with some main components (from Kelly 2002).*

Experimental Setup. The prototype apparatus used was called *megacup* due to the similarity of the measurement principle with ordinary "cups" for water vapor permeability measurements. The megacup is a cylindrical well made of stainless steel (see Figure 2). The inner dimensions of the well are 793 mm (diameter) and 500 mm (depth). The test specimen

is placed horizontally on the top of the chamber. In this way one of the moisture transport forms—convection—could be excluded from the analysis, as the natural convection due to the thermal buoyancy inside the sample was minimized.

On the bottom of the well there is a removable tray with a moisture control unit, climate sensors, fans, and electrical connections. As a part of the moisture controller there is a water flux control system: The mass of a small open water container is weighed with given intervals. As the rest of the inner surfaces of the well are inert, the flux of moisture through the specimen can be determined by the change in the mass of water in the container. The construction details of the megacup are given in Padfield et al. (2002). The steel well is enclosed by an annular outer chamber. Air is circulated in this outer chamber to ensure an even temperature in the well to avoid condensation on the walls. The temperature of this air is controlled by an electric heater and a finned copper tube containing re-circulating cold water. The chamber humidity is controlled by another cold water system, which cools an electrical heat pump. The steel well is well insulated around the periphery and under the bottom plate.

The climate in the chamber, i.e., temperature T and relative humidity RH, and the state of the different elements of the climate control system are measured continuously. A data logger connected to a computer collects the data every minute. An active program analyzes the data and sends control signals to the data logger. The climate inside the megacup can either be constant with respect to both T and RH or oscillating between 10°C and 30°C and 40% and 95% RH. The overall setup is illustrated in Figure 2(b). The lid of the chamber is made of rigid insulation, sealed vapor tight to the chamber wall. In the middle of the lid, there is a square hole of 0.5×0.5 m where the test specimen is placed. The whole

Table 1. Accuracy of the Sorption Equipment

Component	Accuracy
Humidity control	±1% RH (0-90% RH)
	±2% RH (90-95% RH)
Temperature control	±0.05°C
Balance	1 µg

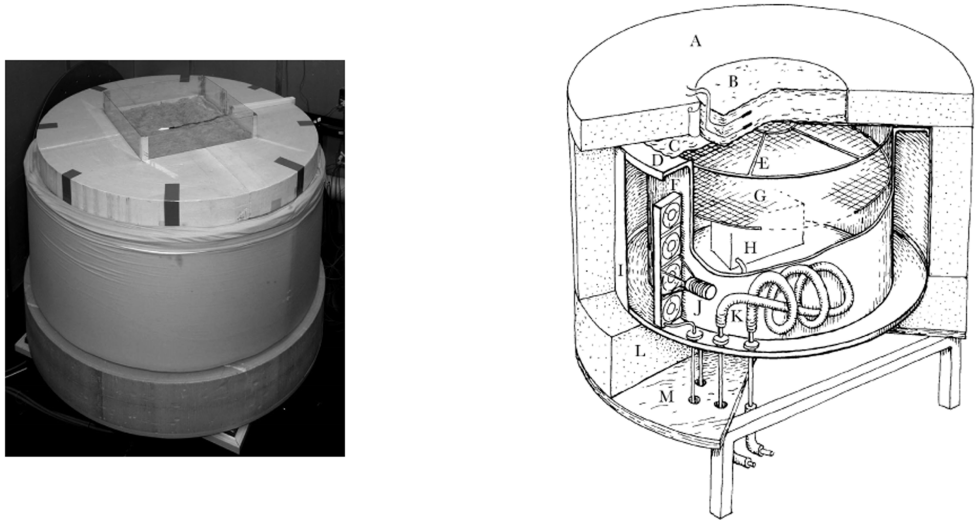

(a) (b)

Figure 2 ***(a)*** *Overall setup with the megacup. The specimen under test is the square piece inserted in the top. All that is visible of the megacup is the exterior insulation.* ***(b)*** *Cross section of the experimental setup and the construction principles: A, thermal guard insulation; B, sample (normally square); C, vapor barrier under the guard insulation; D, flange over annular space; E, open grid; F, fans; G, another grid (not used); H, moisture control unit; I, aluminum wall; J, heating (electric resistance); K, cooling (water circulating in coil); L, bottom insulation; M, table. The illustrations are from Padfield (2002).*

Table 2. Accuracy of the Megacup Equipment and the Sensors Used*

Component	Accuracy
Humidity control	±0.25-1.5%RH
Temperature control	±0.2°C
Moisture flux control	0.001 g
Temperature sensors	±0.2°C
Relative humidity sensors	±1.5% RH (calibrated sensors)

* For humidity control the range in accuracy is due to the different accuracy on different RH levels, the accuracy being best for low RH.

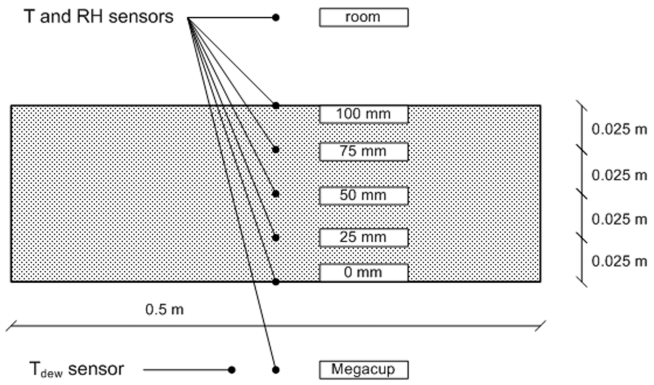

Figure 3 *Location of the temperature and relative humidity sensors within the sample. Dimensions refer to samples with the thickness of 100 mm and sensors on three levels in the sample. Other thicknesses and sensor placements are used, too, but the names of the sensors used for the results are always given in same way—the distance from megacup surface to room. Also, the placement of the* T_{dew} *sensor is given.*

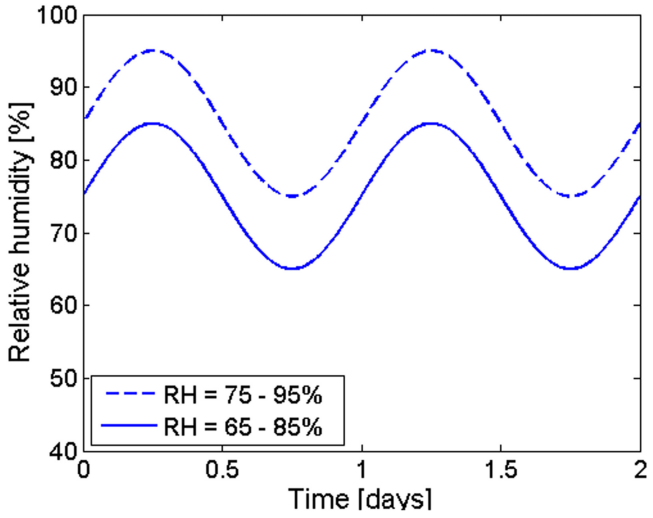

Figure 4 *The sinusoidal variation in the relative humidity of the megacup air* $RH_{Megacup}$. *Only variations 65 < RH < 85% were used for the analysis.*

setup is situated in a climate-controlled room, where temperature and relative humidity can be held constant at the desired levels. The accuracy of the setup is given in Table 2.

In the experiments, small temperature and relative humidity sensors were inserted inside the material at three to four levels and on both surfaces to study the local temperature and moisture distribution (see Figure 3). Temperature was measured by K- and T-type thermocouples. Very small electronic relative humidity sensors (dimensions: 3.8 mm × 8.9 mm × 0.6 mm), which do not disturb the moisture flux, were used. All the RH sensors were individually calibrated, both with respect to relative humidity and temperature.

In this setup the moisture measurements of the material were all by relative humidity sensors. Thus, while one is able to measure the response at different depths into the material, the moisture content of the material cannot be known exactly. Only by assuming that local equilibrium is attained can one approximate the amount of moisture that has participated in the dynamic moisture exchange.

Measurement Strategy. The measurement strategy for the dynamic, non-isothermal tests was to expose a material sample to a sinusoidal change in relative humidity on the cold side with a period of 24 hours (see Figure 4 for the sinusoidal development in $RH_{Megacup}$). There were measurements at two different relative humidity levels: 65 < RH < 85% and 75 < RH < 95% to see if there existed any separate dynamic phenomenon for the high relative humidities. Unfortunately, some unwanted condensation on the inner walls of the megacup was observed when RH > 90%. Therefore, only the relative humidity conditions 65 < RH < 85% were used in the analysis.

The resulting dynamic moisture sorption and transport processes were then surveyed by the built-in temperature and relative humidity sensors.

The sinusoidal relative humidity change and the period at 24 hours were chosen for the following reasons:

1. To illustrate the effect of daily oscillations in relative humidity on the distribution and transport of moisture.

Table 3. Some Material Parameters of the Materials*

Material	Nominal Dry Density (kg/m^3)	Isothermal Permeability (10^{-9}· kg/(Pa·m·s))	
		Dry cup	Wet cup
Glass wool insulation	70	0.18 ± 0.01	0.17 ± 0.006
Rock wool insulation	32	0.16 ± 0.02	0.18 ± 0.03
Aerated cellular concrete	450	0.02 ± 0.001	0.024 ± 0.0004
Cellulose insulation	65	0.13 ± 0.003	0.11 ± 0.002
Flax insulation	30	0.16 ± 0.02	0.15 ± 0.06
Wool insulation	28	0.19 ± 0.02	0.19 ± 0.05
Perlite insulation	100	0.13 ± 0.06	0.10 ± 0.02

* Isothermal permeabilities originate from Hansen (1999), six samples for each condition except for glass wool (three samples) and cellular concrete (four samples) that have been determined as part of this work with the same experimental setup and conditions as in Hansen (1999). Cellular concrete is of the quality sent to several laboratories in Europe, North America, and Japan in 1999 as a part of the CIB W40 TG on material characterization and model bench-marking.

Table 4. Test Sample Dimensions Used in Isothermal Micro-Scale Sorption and Non-Isothermal Megacup Experiments*

Material	Isothermal Tests		Non-Isothermal Tests
	Sample Dry Weight	Sample Size	Sample Thickness
	(mg)	Radius (mm)	(mm)
Glass wool insulation	54.47	6	100
Rock wool insulation	Not measured	Not measured	100
Aerated cellular concrete	113.35	4	100
Cellulose insulation	62.48	6	100
Flax insulation	45.42	7	90
Wool insulation	12.39	5	Not measured
Perlite insulation	50.08	5	140

* Sample shape of the micro-scale tests was close to a sphere with the given radius. Only one sample was used per material

2. A regular and smooth sinusoidal development is easier to analyze than random development as a result of natural climate.

3. In a sinusoidal development, no sudden changes are needed; sudden changes would demand almost unlimited capacity of the moisture control system.

For the sake of simplicity, the temperature was kept constant on both sides of the sample, T_{room} = 22°C and $T_{Megacup}$ = 12°C, and the relative humidity on the warm side was held constant at RH_{room} = 50%. The rationale of having the somewhat high ranges of relative humidity in the chamber was that this was the cold side where the relative humidity would normally be expected to be the highest. The temperature and humidity levels on both sides of the specimen were further chosen such that the vapor pressure gradient in one direction would be opposed by a moisture content gradient in the other direction. This way, the measurement situation could be seen to resemble the type of exposure met in real building enclosures.

Materials

The materials analyzed together with some material parameters and sample dimensions are given in Table 3 and Table 4. All the materials were very porous and relatively lightweight, though very different. They were chosen with the anticipation that their response to a dynamic change in moisture content of the surrounding air would be quite different—some materials would absorb large amounts of moisture, while others would not. The differences in sorption properties can be illustrated by absorption curves given in Figure 5.

Some of these materials are rather common in building envelopes—glass wool and aerated cellular concrete—but some more exotic insulation materials were also included in

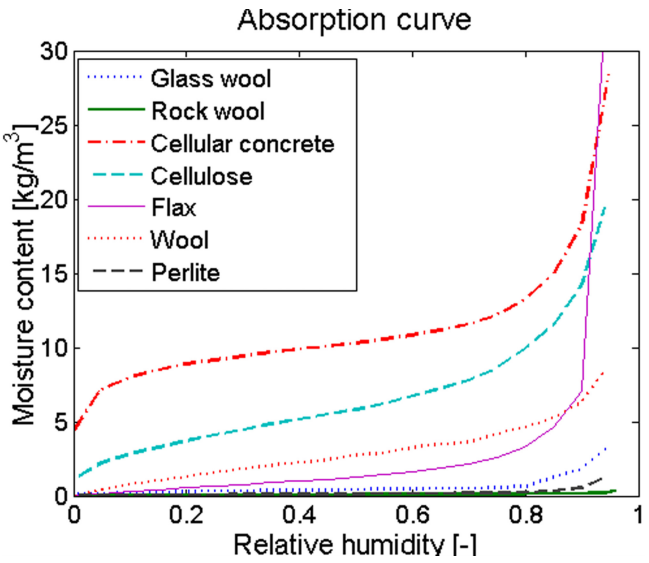

Figure 5 *Absorption curves for the analyzed materials. Sorption isotherms were determined as a part of the isothermal sorption experiments, expect for rock wool insulation, whose values originate from Hansen (1999).*

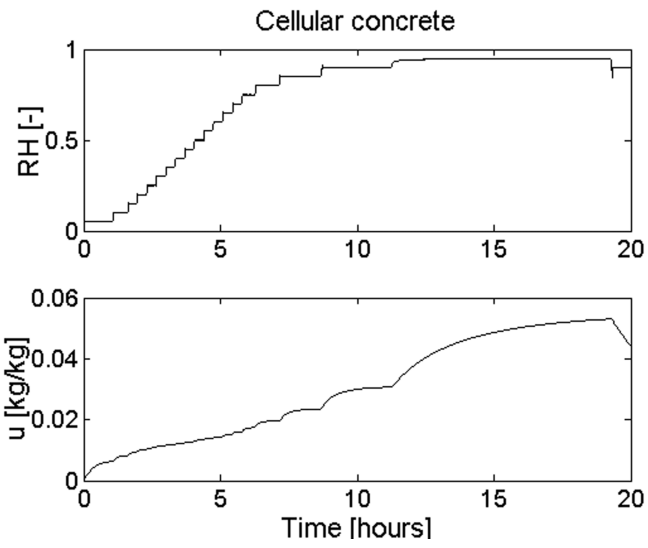

Figure 6 *Consecutive absorption steps for cellular concrete. Relative humidity RH and the resulting moisture content of the material* u *(kg/kg) are given as a function of time.*

the experiments—cellulose, sheep's wool, flax insulation, and expanded perlite. A more detailed description of the investigated materials is found in Peuhkuri (2003).

RESULTS

In the introduction, the theoretical background for moisture buffer capacity of a material in contact with humid air was defined. The current approach could be seen as preliminary to developing a method for determining the moisture buffer capacity using data from the described measurements.

Isothermal Test Results

The kinetic data from the sorption measurements was used in the following analysis of the moisture capacity. An example of a typical sequence is shown in Figure 6, where both the consecutive steps in relative humidity and the resulting weight change of the moisture content of the sample are shown.

Moisture Accumulation Capacity. The moisture buffer capacity expressed as the moisture accumulation capacity is given by Equation 7. Among the involved parameters are two of the most important moisture properties of porous materials, e.g., water vapor permeability δ_p and moisture capacity $\partial w/\partial \varphi$. The validity of use of these steady-state parameters to define a dynamic property such as moisture accumulation capacity b_m will be tested in the following by comparing this theoretical b_m with a dynamically measured b_m, the one given by Equation 10, which is reorganized from Equations 5 and 7. In this way the "dynamic" b_m will not include the steady-state parameter δ_p. Nevertheless, Equation 10 still includes an equilibrium parameter: $\partial w/\partial \varphi$.

$$b_m = \frac{\delta_p}{\sqrt{D_w}} = \frac{\sqrt{D_w} \cdot \frac{\partial w}{\partial \varphi}}{p_{sat}} \tag{10}$$

where the determination of D_w is based on the experimental results from the dynamic sorption measurements and on the assumption of sorption rates for a slab with a half-thickness of l (m) according to Crank (1975). The following expression for D_w (Equation 11) is widely used by several researches, e.g., Künzel and Kiessl (1990) and Wadsö (1993), when studying the initial sorption rates, $E < 0.5$.

$$D_w = \frac{\pi}{4} \cdot l^2 \left(\frac{dE}{d\sqrt{t}} \right)^2 \tag{11}$$

where the nondimensional moisture content E, as an average over the thickness of the sample, is defined as in Equation 12.

$$E = \frac{w(t) - w(0)}{w(\varphi) - w(0)} \tag{12}$$

where $w(t)$ is moisture content at time t, $w(0)$ is moisture content at $t = 0$, and $w(\varphi)$ is the equilibrium moisture content by the target relative humidity φ.

Figure 7(a) shows the buffer capacity as moisture accumulation capacity b_m according to Equation 7 as a function of relative humidity, i.e., "steady state" b_m. The trend of b_m was very similar for all materials, i.e., b_m was lowest for moderate

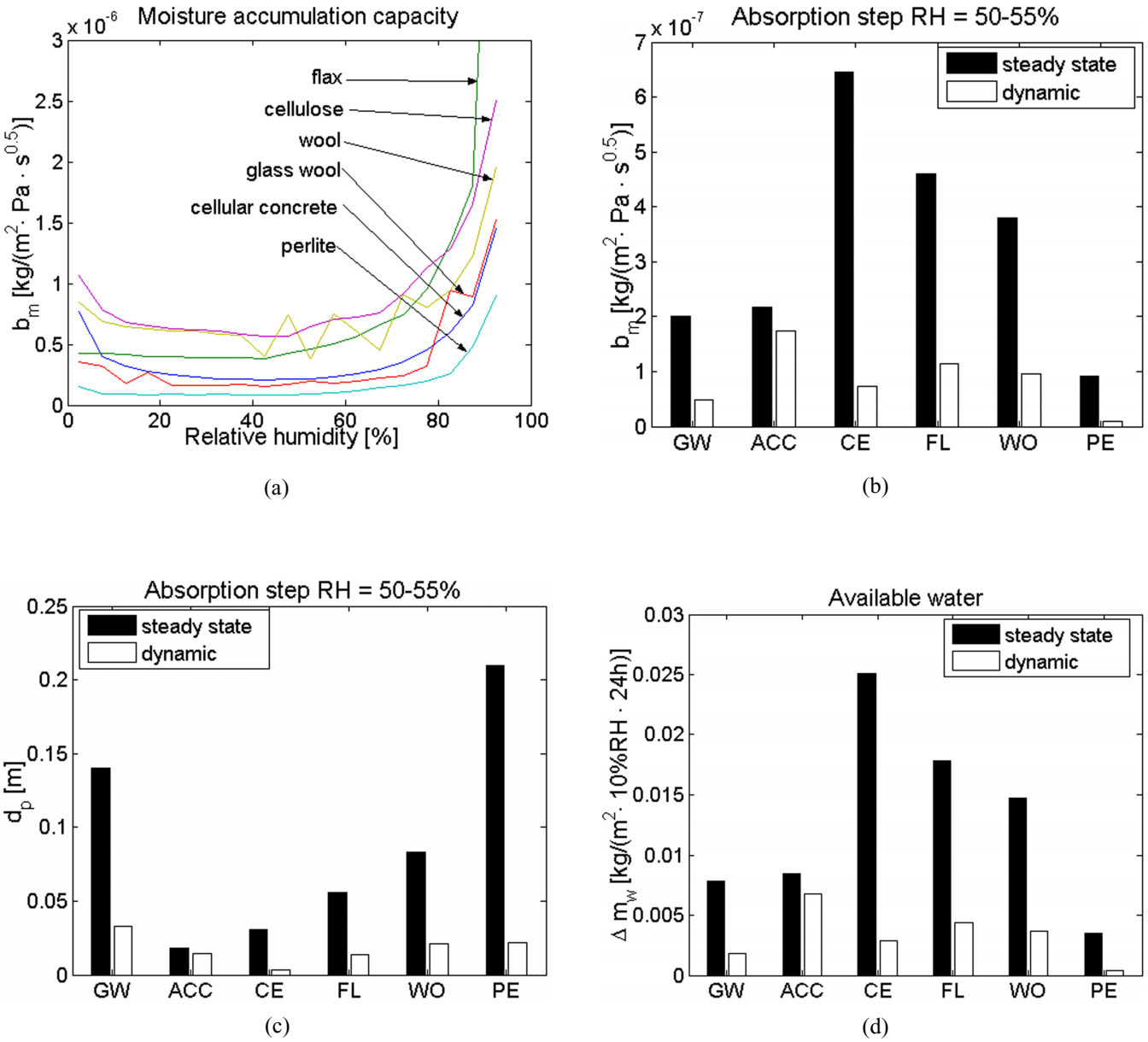

Figure 7 ***(a)*** *Moisture accumulation capacity* b_m *(kg/(Pa·m²·s^0.5)) as a function of relative humidity. Steady-state parameters (Equation 7).* ***(b)*** b_m *and the significance of the analysis method. Comparison of* b_m *with steady-state and dynamic approach. Absorption step RH = 50-55%.* ***(c)*** *Penetration depth* d_p *determined from steady-state and dynamic measurements.* ***(d)*** *Comparison of available water* Δm_w *([kg/m² per* $\Delta\varphi = 0.1$ *and* $t_p = 24$ *hours) for the absorption step RH = 50-55% between steady-state and dynamically determined* d_p*. GW = glass wool, ACC = cellular concrete, CE = cellulose insulation, FL = flax insulation, WO = sheep's wool, and PE = perlite.*

RHs, where the slope of the sorption isotherm was also smallest, and increased for increasing (and decreasing) RH.

Figure 7(b) illustrates the big difference in magnitudes between the two methods analyzed, i.e., "steady state" and "dynamic" b_m. In general b_m was much smaller when the dynamic method was applied than when the steady-state parameters were used. An exception was cellular concrete, where the two determined values for b_m were practically equal.

Available Water. Another way of presenting the buffer capacity is to determine the amount of available water for given changes in ambient RH. This method is given with Equation 9. It is not indifferent how the moisture diffusivity for determining d_p, and the moisture capacity $\partial w/\partial\varphi$ of the

materials are determined. If diffusivity is determined from steady-state permeability (Equation 5), d_p will be overestimated compared to the dynamic case [see Figure 7(c)]. The dynamically measured diffusivity from the previous section turned out to be smaller than the one that could be determined from Equation 5 due to the small slope of the measured nondimensional moisture content versus the square root of time.

Therefore, a distinction was made between a d_p determined by steady state and a dynamically determined d_p. The latter was determined with Equation 8, where D_w was derived from the dynamic sorption measurements. The steady-state d_p was determined from Equation 13, which is based on Equations 5 and 8. These resulting penetration depths are shown in Figure 7(c) for a step RH = 50-55%.

$$d_p = \sqrt{\frac{\delta_p \cdot p_{sat} \cdot t_p}{\frac{\partial w}{\partial \varphi} \cdot \pi}} \tag{13}$$

Overall, the picture was identical for Δm_w as for b_m, when assessing the analyzed materials; see Figure 7(d). This was not a surprise as these values were proportional; see Equation 14. Δm_w just gave a more realistic idea of the amounts of moisture involved during a typical period (here 24 hours) and for a given change in RH (here ΔRH = 10%, $\Delta\varphi$ = 0.1).

$$\Delta m_w = b_m \cdot p_{sat} \cdot \Delta\varphi \sqrt{\frac{t_p}{\pi}} \tag{14}$$

Equation 14 gives the close coupling between the moisture accumulation capacity b_m and the amount of water Δm_w that is exchanged in a situation with periodically varying conditions. Thus, while moisture accumulation capacity could be a good figure of merit for a material's intrinsic moisture buffering property, available water may be more appropriate to use (and understand) as a design parameter when a specific cycle, e.g., 24 hours, is of interest. In this context, it is also interesting to note the square root of time dependency of available water, which makes it possible to recalculate into effects on other time scales.

Moisture Capacity—Slope of Sorption Curve. Finally, after it was clear that the moisture buffer capacity followed, at least to some extent, the well-known characteristics of the slope of the sorption isotherm, also called moisture capacity, it was interesting to assess if this definition of moisture capacity could be used for the sake of simplicity. Moisture capacity is given here as the volumetric moisture capacity $\partial w/\partial\varphi$, and the "ranking" of the assessed materials is shown in Table 5.

The characteristics here are pretty much equal to the two earlier definitions: moisture buffer capacity is largest for high RHs. But the "order" of the materials is not identical with the other moisture buffer definitions, neither with the ones with steady-state nor with dynamic parameters. Therefore, this traditional definition of moisture capacity cannot be used, at least for the analyzed materials. The main reason for this deviation compared to b_m (and Δm_w) is that this "simple" moisture capacity does not take into account the transport rate of moisture at all. The moisture capacity given by the sorption isotherm is an equilibrium value, and, therefore, not all the capacity will become activated in the dynamic moisture buffering case. In addition, the moisture capacity $\partial w/\partial\varphi$ of some materials, such as flax and cellular concrete, was extremely high for high relative humidities and, therefore, does not give the right picture of the buffer performance of the materials.

It was not indifferent which equation was used for the "ranking" of the assessed materials. In Table 5, the materials are ranked for the interval 50-55%RH. The materials are ranked according to the three terms (Equations 7 and 10) and $\partial w/\partial\varphi$) with the material with largest moisture accumulation capacity mentioned first. A more detailed analysis of the effect of the relative humidity levels is found in Peuhkuri (2003).

Non-Isothermal Test Results

For the following analysis, the dynamic temperature and relative humidity distribution within the material was used. An example of a measurement sequence is shown in Figure 8.

Penetration Depth. The differences between the materials and the method of analysis will be demonstrated here by determining their penetration depth, both as a measured value and a theoretical value. These depths in Table 6 are valid for RH = 65-85%, which was the sinusoidal variation of the air humidity on the cold side (12°C).

Table 5. Difference Between the Analysis Methods—Measured Materials are Given in Order Where the One with the Highest Moisture Buffer Capacity is Number 1

	Steady-State Parameters, Equation 7	Dynamically Determined D_w, Equation 10	"Simple" Moisture Capacity, $\partial w/\partial\varphi$
1	Cellulose insulation	Cellular concrete	Cellulose insulation
2	Flax insulation	Flax insulation	Cellular concrete
3	Sheep's wool	Cellulose insulation	Flax insulation
4	Cellular concrete	Sheep's wool	Sheep's wool
5	Glass wool	Glass wool	Glass wool
6	Perlite	Perlite	Perlite

Table 6. The Measured and Theoretical "Penetration Depth" d_p for Non-Isothermal, Sinusoidal Oscillations in the Megacup (RH = 65-85%)*

Material	Penetration Depth [*mm*]	
	Measured	Theoretical
Glass wool	55	52
Rock wool	>100	104
Cellular concrete	32	9
Cellulose	37	18
Flax	35	27
Perlite	85	90

*The measured d_p is a result of fitting the measured vapor pressure distribution with the theoretical solution for a slab according to Equations 15 and 16. The penetration depth was defined as a depth from the cold side, where the oscillations in RH were 36.7% of the oscillations on the material surface, here the cold side. The theoretical d_p was determined from Equation 13.

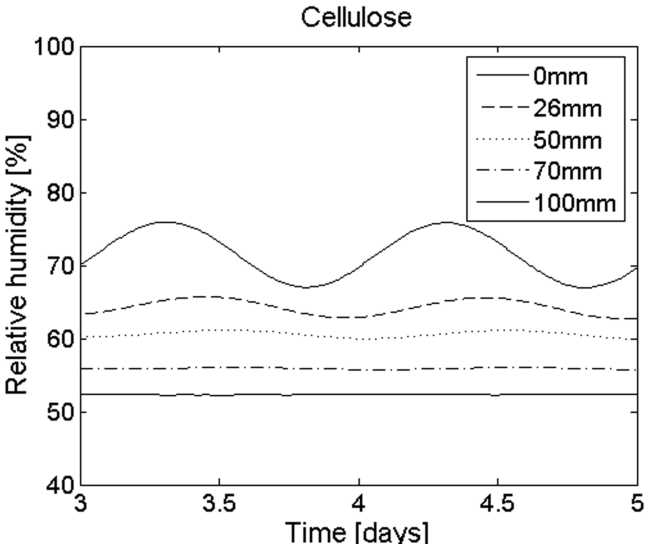

Figure 8 *The measured distribution of relative humidity in cellulose insulation for sinusoidal variation RH = 65-85% of the air on the cold side of the test sample.*

The "measured" d_p is determined on the basis of theory for periodic solutions for temperature in a homogenous slab according to Hagentoft (2001). An analogy between temperature and vapor pressure—and the superposition principle—is used in the present analysis. Vapor pressure p can be calculated from the measured T and RH.

The cold surface is exposed to a sinusoidal variation $p_{1,t}$, which is the measured p on the surface *minus* the average p_{mean}. The warm side of the slab with a thickness d is kept at the constant p_2, which is the average of the measured values. The distribution of the $p_{x,t}$ as a function of distance x and time t is determined with Equations 15 and 16.

$$p_{1,t} = p - p_{mean} \tag{15}$$

$$p_{x,t} = p_{1,t}\frac{\sinh\left[(1+i)\frac{d-x}{d_p}\right]}{\sinh\left[(1+i)\frac{d}{d_p}\right]} + p_{mean} + \frac{x}{d}(p - p_{mean}) \tag{16}$$

This calculated p distribution is then given as RH by using the theoretical distribution of temperature in the same way as in Equations 15 and 16. The "measured" d_p is determined by fitting the resulting RH distribution with the measured distribution until they agree to defined accuracy. Theoretical d_p is defined from Equation 13.

The main observation was that the "measured" penetration depth d_p, defined as a measure for the sinusoidal oscillations, being less than 36.7% of the oscillations on the cold surface of the material at this location, was largest for rock wool and perlite and smallest for materials such as cellular concrete, cellulose, and flax insulation. This means that the material that was on the "warm side" of this depth could only "feel" about one-third of the changes in the relative humidity in the megacup or less. Subsequently, within this "inactive" part of the materials there existed almost steady-state conditions in terms of moisture absorption and desorption. The measured RH range involved inside the material during a period of 24 hours is illustrated in Figure 9 for cellulose, together with the "measured" and theoretical penetration depth.

The theoretical d_p is significantly smaller than the "measured" one for cellular concrete and cellulose insulation, and there is some difference for flax. For glass wool, rock wool, and perlite, there is almost no difference.

Buffer Capacity. Penetration depth, given in Table 6, can be used to give an indication of how much moisture is involved in the dynamic moisture transport process, together with the moisture capacity. Consequently, materials with a large penetration depth and a high moisture capacity involve lots of moisture under a dynamic absorption and desorption process while the reverse holds true for materials with small penetration depths and poor moisture capacity.

The buffer capacity of the materials determined as the moisture accumulation capacity b_m (kg/(m²·Pa· s$^{0.5}$)) was theoretically given by Equation 7. By rearranging, this equation can be expressed as Equation 17, which includes the "measured" d_p. In this way the moisture accumulation capacity b_m can also be given as a "measured" value. Both the theoretical and the measured values for b_m are given in Table 7 and in Figure 10.

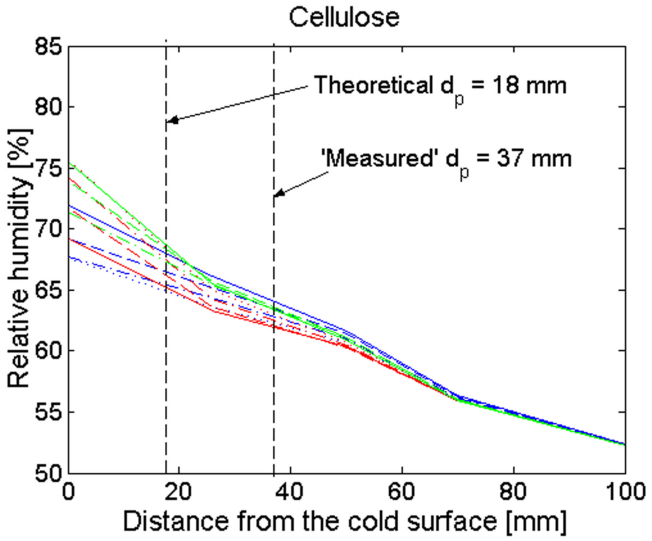

Figure 9 *The measured relative humidity as a function of distance from the cold surface for sinusoidal variation in the megacup 65-85% RH for cellulose insulation. The different curves are values for different times during a 24-hour period. Also, the "measured" and theoretical penetration depths are given.*

$$b_m = \frac{d_p \cdot \frac{\partial w}{\partial \varphi}}{p_{sat}} \sqrt{\frac{\pi}{t_p}} \qquad (17)$$

The moisture buffer capacity given as available water Δm_w (kg/m^2 per $\Delta\varphi = 0.1$ and $t_p = 24$ hours) (Equation 9) is also calculated as both a theoretical and a "measured" value. The d_p for the "measured" case is the measured value and the theoretical d_p for the theoretical case is given in Table 6. These theoretical and "measured" values for Δm_w are compared in Table 8. The moisture capacity $\partial w/\partial \varphi$ in both cases is still determined from the equilibrium moisture content.

DISCUSSION AND CONCLUSION

The ability of some insulation materials to serve as moisture buffers for changes in ambient relative humidity has been assessed analytically and experimentally. The analysis was undertaken with results from both isothermal and non-isothermal dynamic tests. The importance of the choice of the material parameters for the resulting moisture buffer capacity based on parameters determined either from steady state or dynamically was also pointed out. Different methods were presented to define an expression that could indicate a material's ability to buffer for changes in ambient relative humidity based on dynamic measurements vs. standard (=steady-state) material parameters. The methods "ranked" the materials in more or less the same order, but it was not indifferent if the parameters were determined from steady-state or dynamic measurements, or what method was used. Therefore, when using steady-state parameters and when comparing the resulting moisture buffer capacity with results from isothermal step measurements, the moisture buffer capacity was overestimated compared to the dynamic case where determined moisture diffusivity was used. On the other hand, when using steady-state parameters and when comparing the resulting moisture buffer capacity with results from non-isothermal dynamic measurements and using the "measured" penetration

Table 7. Theoretical and "Measured" Values for Moisture Accumulation Capacity b_m*

	Volumetric Moisture Capacity	Moisture Accumulation Capacity b_m	
	(kg/m³)	(10^{-7} kg/(m²·Pa· s$^{0.5}$))	
Material	Average	Measured	Theoretical
Glass wool	3.8	6	5
Rock wool	0.24	3	3
Cellular concrete	19.0	17	5
Cellulose	21.2	20	10
Flax	13.7	12	9
Perlite	0.77	2	2

* Theoretical values are calculated from Equation 7 and the "measured" ones from Equation 17. The slope of the sorption isotherm is determined from the isothermal sorption experiments presented in Figure 5 and given here as the volumetric moisture capacity $\partial w/\partial \varphi$. The "measured" penetration depth is given in Table 6. Values are valid for RH = 65-85%.

Table 8. The Available Water Δm_w Calculated from Equation 9*

Material	Available Water Δm_w (g/(m²· 10%RH·24h))	
	Measured	Theoretical
Glass wool	22	21
Rock wool	11	11
Cellular concrete	65	18
Cellulose	78	39
Flax	48	36
Perlite	7	7

* The slope of the sorption isotherm is determined from the isothermal sorption experiments. Penetration depth is measured from the non-isothermal tests in the Megacup given in Table 6. These dynamic, non-isothermal values are compared with the theoretical values based on the theoretical d_p given by Equation 13. ΔRH=10% has been chosen as an arbitrary value for comparison. Values are valid for RH = 65-85%.

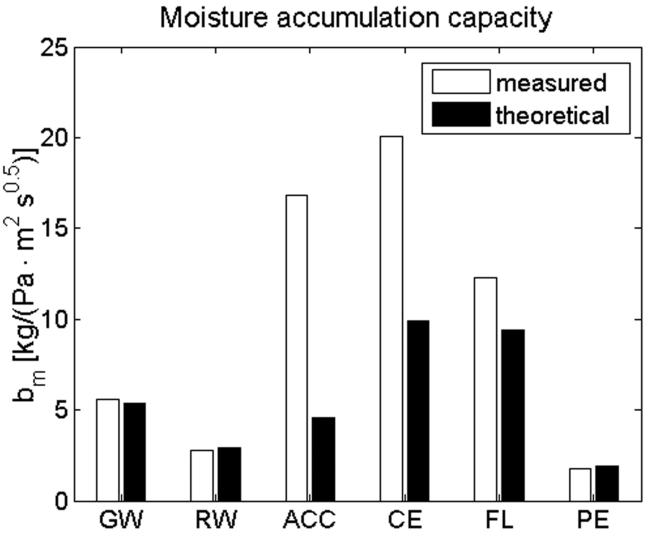

Figure 10 *Theoretical and "measured" values for moisture accumulation capacity* b_m *for all the measured materials. Values are valid for RH = 65-85%.*

depth for the dynamic case, the moisture buffer capacity was underestimated for those materials with good buffer capacity, e.g., flax and cellulose insulation and cellular concrete, while there was no difference for materials with poor buffer capacity, such as glass wool, rock wool, and perlite.

The observations on the high moisture buffer capacity of absorbent insulation materials in the present analysis support the findings in Padfield (1999), for example.

The use of relative humidity sensors to measure the moisture conditions within and around the specimens is based on the assumption of local equilibrium, where the relative humidity in the pores of a porous material is in equilibrium with the water content of the material. As already discussed, this assumption is not necessarily correct under dynamic conditions, or in steady state, due to hysteresis. The measurement strategy was based on dynamic conditions. Therefore, the local moisture content could not be fully estimated with the relative humidity sensors used.

What does this buffer capacity of the materials actually mean? The answer is that materials with a large buffer capacity, such as cellulose, flax insulation, and cellular concrete, should be able to moderate the oscillations in the relative humidity. Oscillation in relative humidity in a building as such is usually not dangerous, but high oscillation often also means high peaks in relative humidity. Consequently, constructions composed of materials with a good buffer capacity can be expected to be more resistant to damage due to high moisture loads than constructions with, e.g., mineral wool and perlite.

The same damping effect of oscillations is also expected for the indoor air relative humidity. However, it must be stressed here that the moisture buffer capacity of the analyzed insulation materials only refer to the conditions *inside* a construction because in normal applications the insulation will be hidden behind interior claddings or surface coatings and possibly a vapor retarder.

Nevertheless, the methodology will be the same, regardless of whether one analyzes the humidity of the indoor air or the inner layers of the constructions.

As a main conclusion of the study it can be stated that there is need for a standard for the characterization of the dynamic response of materials; the results are too sensitive to the chosen analysis method and will depend greatly on the choice. A project to define the moisture buffer capacity of building materials has been started within the NORDTEST organization by a group of international experts (see Rode et al. [2003] for information about a preliminary workshop on the project and its topic). Another project where moisture buffer capacity of materials will be put in context with the prediction and design of hygrothermal conditions of building enclosures and indoor air quality is IEA Annex 41, Whole Building Heat, Air and Moisture Response (Hens 2003).

ACKNOWLEDGMENTS

This paper presents a minor part of the results of the Ph.D. thesis of Ruut Peuhkuri (Peuhkuri 2003) with Associate Professors Carsten Rode and Kurt Kielsgaard Hansen as supervisors.

Most of the sorption experiments with the standard sorption apparatus were carried out during a research stay at Glasgow Caledonian University, School of Engineering, Science and Design. Many thanks to Professor Graham Galbraith and his staff, especially to Dr. David Kelly and David Bailly, who completed the sorption measurements after the end of the stay. The stay was funded by a grant from the Larsen & Nielsen Foundation.

The prototype non-isothermal apparatus was mostly designed by Dr. Tim Padfield (Padfield et al. 2002). Special thanks to him for his prompt problem solving when running the equipment

REFERENCES

Crank, J. 1975. *The Mathematics of Diffusion*. Oxford: Clarendon Press.

Fick, A. 1855. *Über Diffusion. Annalen der Physik und Chemie*, vol. 94, pp. 59-86.

Hagentoft, C.-E. 2001. *Introduction to Building Physics*. Studentlitteratur.

Hansen, E.J., K.K. Hansen, and T. Padfield. 1999. Measured moisture properties for alternative insulation products. *Proceedings of 5th Symposium on Building Physics in the Nordic Countries, Göteborg*.

Hedegaard, L. 2002. Moisture buffer capacity of building materials (in Danish). Master's thesis. Department of Civil Engineering, Technical University of Denmark.

Hens, H.S.L.C. 2003. Proposal for a new Annex: Whole building heat, air and moisture response (MOIST-ENG). 2nd draft.

Håkansson, H. 1998. Retarded sorption in wood. Ph.D. thesis (Report TABK-98/1012), Department of Building Science, Lund Institute of Technology, Lund University.

Kelly, D.J. 2002. Rapid experimental methods for the evaluation of material moisture permeability. Ph.D. thesis, School of Built and Natural Environment, Glasgow Caledonian University.

Koponen, S., and L. Liu. 1999. Modeling of moisture transfer in wood based on cell structure. *Proceedings of 5th Symposium on Building Physics in the Nordic Countries. Göteborg*.

Künzel, H.M., and K. Kiessl. 1990. Bestimmung des Wasserdampfdiffusionswiderstandes von mineralischen Baustoffen aus Sorptionsversuchen. Bauphysik 12.

Mitamura, M., C. Rode, and J.M. Schultz. 2001. Full scale testing of indoor humidity and moisture buffering in building materials. Proceedings of *IAQ 2001*. San Francisco.

Ojanen, T., and M. Salonvaara. 2003. A method to determine the moisture buffering effect of structures during diurnal cycles of indoor air moisture loads. *Proceedings of 2nd International Conference on Building Physics. Leuven.*

Padfield, T. 1999. The role of absorbent building materials in moderating changes of relative humidity. Ph.D. thesis (Report no. 54), Department of Structural Engineering and Materials, Technical University of Denmark.

Padfield, T., R. Peuhkuri, C. Rode, and K.K. Hansen. 2002. Non-isothermal water vapour transmission through porous insulation. Part 1: Equipment. *Proceedings of 6th Symposium on Building Physics in the Nordic Countries. Trondheim*.

Peuhkuri, R. 2003. Moisture dynamics in building envelopes. Ph.D. thesis, Department of Civil Engineering, Technical University of Denmark.

Rode, C. 2003. Workshop on Moisture Buffer Capacity—Summary Report. Report No. 67, Department of Civil Engineering, Technical University of Denmark.

Wadsö, L. 1993. Studies of water vapor transport and sorption in wood. Ph.D. thesis, Department of Building Science, Lund Institute of Technology, Lund University.